

# Development of a Real Time Front-End Time-Domain Calibration System for the Advanced LIGO Detectors

Craig Cahillane

Caltech LIGO SURF 2013

Mentors: Alan Weinstein and Jameson Rollins

September 25, 2013

## Abstract

The Advanced LIGO gravitational wave detectors are currently under construction along with new, more precise calibration control systems. Our goal is to understand the Advanced LIGO detectors response to incident gravitational waves. During detector operation, parameters characterizing the detector can change in real time, altering the detectors response to gravitational waves. These changes in the detector response must be tracked and taken into consideration when calibrating gravitational wave strain. We propose instituting a real time front-end time-domain calibration system in order to better track the changes of the detector response during science runs. Development of such a calibration system is underway at the Caltech 40m interferometer.

## 1 Introduction

The Laser Interferometer Gravitational-Wave Observatory (LIGO) is a network of three detectors built to detect local perturbations in the space-time metric known as strain from astrophysical sources. The anticipated size of these perturbations is  $10^{-23}$ m, less than one ten-thousandth of the diameter of a proton. [4] Extreme care is taken to shield the detectors from noise, but not all noise can be prevented. This means true gravitational wave strain is difficult to discern due to low signal-to-noise ratio. Calibration allows us to measure how the detector will respond to an incident gravitational wave strain.

### 1.1 Advanced LIGO Detectors

At the heart of the Advanced LIGO detectors resides a dual-recycled Fabry-Perot Michelson interferometer. A Michelson interferometer consists of a laser beam fired into a beam splitter, allowing half of the laser light straight through

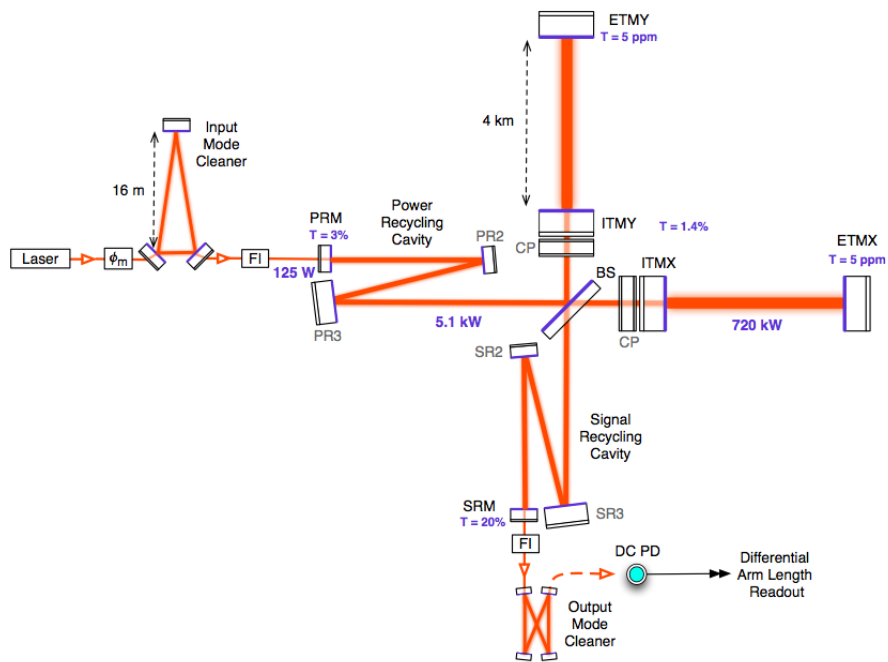


Figure 1: Advanced LIGO Michelson Interferometer diagram. The ETM and ITM form the Fabry Perot cavities, while the three PRM and two ITM form the power recycling cavity. If both arms are an integral number of wavelengths of laser light, then all carrier light in the Signal Recycling AS port destructively interferes and the interferometer is said to be “on resonance”. Image from [4]

and deflecting the other half 90 degrees. The light in the interferometer is phase modulated to produce Radio Frequency (RF) sidebands at  $\omega_m \approx 2\pi \times 25$  MHz. The original frequency of light, called the carrier frequency, is tuned for constructive interference within the Fabry-Perot cavities. The sideband frequencies are not tuned to resonate in the Fabry-Perot cavities, and instead reside largely in the Power Recycling Cavity and Signal Recycling Cavity to aid in signal extraction.

The carrier light travels in perpendicular arms of nearly the exact same length until it hits a reflecting mirror. This reflected light carries back with it a phase difference based on the microscopic difference in length of each arm. This difference in the arm lengths is known as the differential arm length, or DARM. When the DARM is zero, there is no phase difference in the light, and by destructive interference no carrier band light enters the photodiode at the Antisymmetric (AS) port. When there exists a phase difference in the light, we can detect the optics' movement by detecting carrier band light beating with the sideband light frequencies in the AS port. [5] This change in the DARM length includes both noise and astrophysical strain signal.

## 1.2 Feedback Control Loop

A feedback loop keeps the interferometer in its resonance condition. Resonance condition is when the distance between the mirrors of the interferometer is an integer value of the wavelength of laser light in the interferometer. When this occurs, the reflected light constructively interferes in the power recycling cavity and destructively interferes in the signal recycling cavity, or the AS port. This resonance condition is maintained by a servo actuator that responds to a digital error signal  $e_D(f)$ .  $e_D(f)$  is proportional to the DARM length change  $\Delta L_{ext}(f)$  and feedback actuation length  $\Delta L_A(f)$ . The error signal  $e_D(f)$  is the result of the digitization of the analog signal registered by the interferometer, and, most important, it has a linear relationship when in resonance condition:

$$\Delta L_{ext} = R_L(f)e_D(f) \tag{1}$$

where  $R_L(f)$  is the response function. In the long wavelength approximation,  $\Delta L_{ext}$  is linearly related to gravitational wave strain  $h(f)$ :

$$h(f) = \frac{\Delta L_{ext}}{L} \tag{2}$$

where  $L$  is the measured length of the arm cavities. Finding this linear response function is a process known as frequency-domain calibration. [1] [3]

We want to preserve the linear relation between  $e_D(f)$  and gravitational strain  $h(f)$ , so feedback control loops are used to keep DARM close to zero. In this linear domain we must measure the response function  $R_L(f, t)$  accurately to get an accurate strain signal.

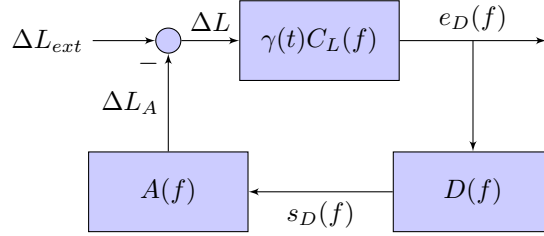


Figure 2: Visualization of the Feedback Control System Loop. The interferometer senses a change in the DARM length  $\Delta L_{ext}$  and receives feedback input  $\Delta L_A$ , producing a digital error signal  $e_D(f)$ . The digital filters  $D(f)$  produce a digital control signal  $s_D(f)$ . Finally, the actuation function  $A(f)$  determines the motion necessary to keep the interferometer in its resonance condition, sending a new actuation  $\Delta L_A$ .

The response function  $R_L(f, t)$  depends on the sensing function  $C_L(f)$ , digital filters  $D(f)$ , and actuation function  $A(f)$  in the following relationship:

$$R_L(f, t) \equiv \frac{1 + \gamma(t)G_L(f)}{\gamma(t)C_L(f)} \quad (3)$$

where  $\gamma(t)$  is the slow time dependence of the sensing function's  $C_L(f)$  and  $G_L(f) = C_L(f)D(f)A(f)$  is the open loop gain.

$R_L(f)$  is important because the convolution kernel  $R_L(t - t')$  can be reproduced from it, and this convolution kernel is used to reconstruct the gravitational strain  $h(t)$  in the equation:

$$h(t) = \frac{1}{L} \int R_L(t - t') e_D(t') dt' \quad (4)$$

The open loop gain  $G_L(f)$  is separated into three components:  $G_L(f) = C_L(f)D(f)A(f)$ . Each of these three components is crucial to the overall response function of the detector.  $C_L(f)$ , the sensing function, captures the analog  $\Delta L_{ext}(f)$  and converts it into a digital signal  $e_D(f)$ . A photodiode detects how much carrier light reaches the AS port, which determines  $\Delta_{ext}L(f)$ , then runs this analog signal through the sensing function  $C_L(f)$ , here approximated to a single cavity pole transfer function:

$$C_L(f) \approx \frac{1}{1 + i \frac{f}{f_c}} \quad (5)$$

where  $f_c$  is the cavity pole frequency and  $i$  is the imaginary unit. [4] [1]  $D(f)$ , the digital filter, converts  $e_D(f)$  into a digital control signal  $s_D(f)$  to be sent back to the detector mirror.  $A(f)$ , the actuation function, converts  $s_D(f)$  into an analog signal that physically moves the mirrors. In Initial LIGO, the mirrors

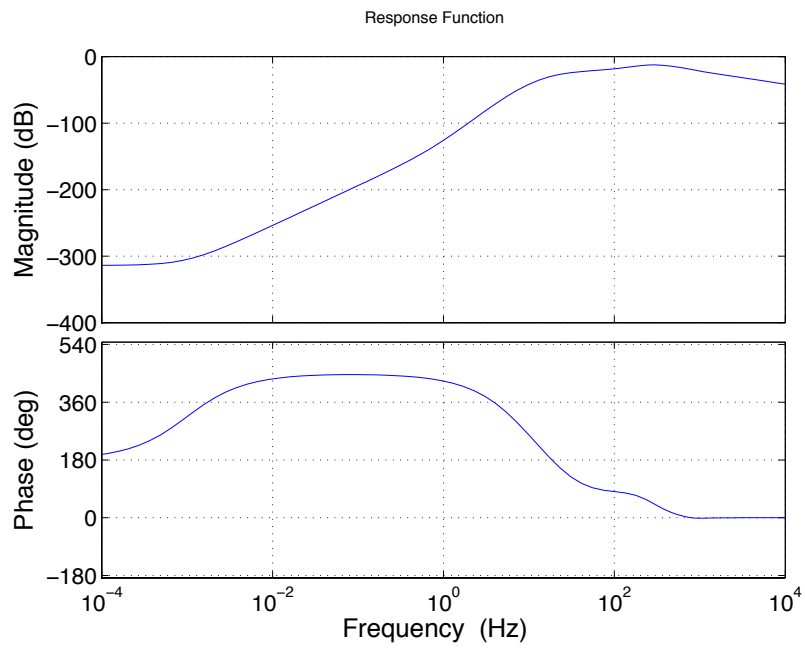


Figure 3: Response Function Bode Plot. The response function  $R_L(f)$  plotted with respect to frequency. In the linear resonance condition, we multiply this function by  $e_D(f)$  to get  $h(f)$ , the GW strain in the frequency domain. This plot created with parameters from Hanford interferometer H1 in S5. [1]

that reflect the laser light are pendulums, and the pendulums' natural frequency response yields a good approximation for the complete actuation function:

$$A(f) \approx \frac{1}{f_p^2 - f^2 + i\frac{f_p f}{Q}} \quad (6)$$

where  $f_p$  is the natural frequency of the pendulum and  $Q$  is the quality damping factor. [4] [1]

From Figure 3, we see two different signals can be used to reconstruct  $\Delta L_{ext}$ : the error signal  $e_D(f)$  and control signal  $s_D(f)$ . From Equations (1) and (3), ignoring the factor  $\gamma(t)$ , we get

$$\Delta L_{ext} = \frac{1+G}{C_L} e_D \quad (7)$$

$$\Delta L_{ext} = A \frac{1+G}{G} s_D \quad (8)$$

### 1.3 Method of Calibration

The properties of the open loop gain  $G$  at certain frequencies make the use of both of these signals essential. As frequency  $f$  goes to zero, the open loop gain  $G$  goes to infinity, causing Equation (7) to blow up at low frequencies. Alternatively, as frequency  $f$  goes to high frequency  $G$  must go to zero to keep the loop stable. This causes Equation (8) to blow up. However, we can combine the two, using the control signal at low frequencies and the error signal at high frequencies:

$$\begin{aligned} \Delta L &= \Delta L_{ext} - \Delta L_A \\ \Delta L_{ext} &= \Delta L + \Delta L_A \end{aligned}$$

From Figure 2 we can see that  $\Delta L = \frac{e_D}{C_L}$  and  $\Delta L_A = s_D A$ , giving

$$\Delta L_{ext} = \frac{e_D}{C_L} + s_D A \quad (9)$$

From Equation (9) we see that this method of strain reconstruction completely avoids the digital filters  $D$ , allowing for changes to the filters to be made in real time with no repercussions to our calibration.

### 1.4 Time Domain Calibration

During detector operation, parameters critical to the calibration can change in real time. For example, the optical gain of each cavity tends to fluctuate while the detector is taking data. For Advanced LIGO we want to track the system changes in real time more closely. In order to do this we want to implement a time-domain calibration system at the front end, so changes in the detector response are immediately found and accounted for. We must first check if the time-domain system can give us a better calibration and quantify the errors in

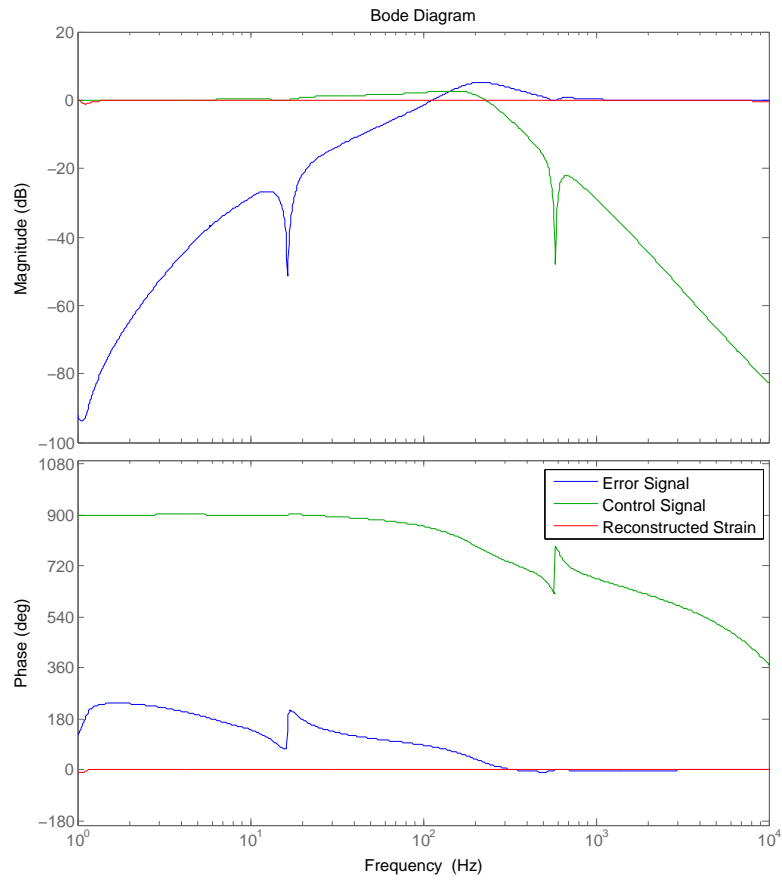


Figure 4: Reconstruction of Strain in the Frequency Domain from the Error and Control Signals. The strain magnitude levels at zero decibels, giving near perfect signal reconstruction capabilities from this method. [6]

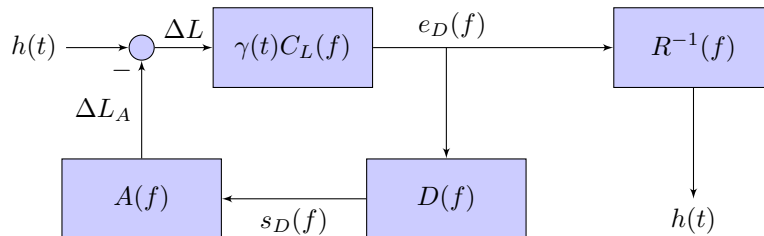


Figure 5: Reimagined 40m Interferometer Feedback Control System. The inverse response function  $R^{-1}(f)$  immediately takes the error signal  $e_D(f)$  and converts it to the strain signal  $h(t)$  sensed by the interferometer in the time domain. This occurs before on the “Front End”, before the digital filters  $D(f)$  alter the signal.

its calculation. If the time-domain system proves to be useful, it can potentially reduce our uncertainty in the gravitational wave strain  $h(t)$ . [2]

In the case of an interferometer, we want to convert counts into meters representing the DARM displacement. For a time domain calibrator, we will run the inverse of the linear response function  $R^{-1}(f)$  on the error signal  $e_D(f)$ , producing the strain signal  $h(t)$ . But the response function is changing in real time, so we must measure how  $R(f)$  and  $R^{-1}(f)$  are changing and adjust them accordingly. To do this in real time, calibration lines are input into the interferometer at specified frequencies of known magnitude and phase. The calibrator will demodulate at the calibration line frequencies and analyze how the signal has changed due to changes in the response function. From this information, we should be able to construct the inverse response function  $R^{-1}(f)$  as it changes in time.

The calibration code was written in MATLAB and Simulink, using tools for linear time domain filtering. Our model focused only on the DARM interferometer configuration which is sensitive to gravitation waves.

## 2 Progress

I worked on understanding the aLIGO control system Simulink models made by Jeff Kissel and Rana Adhikari. I attempted to implement Equation (9) in a Simulink block subsystem within Adhikari’s model to replicate strain in the frequency domain. However, inverting the sensing function  $C_L$  is very difficult in Simulink due to instabilities. Simulink will only simulate physical, causal systems: In particular, Simulink does not allow systems with more zeros than poles in their transfer functions to be implemented.

To combat this problem, we have introduced artificial poles at 8 kHz to the inverse sensing function in order to create a stable system that Simulink accepts. These additional poles cause a downturn in the response around 8 kHz, but are necessary to create a physical control system.



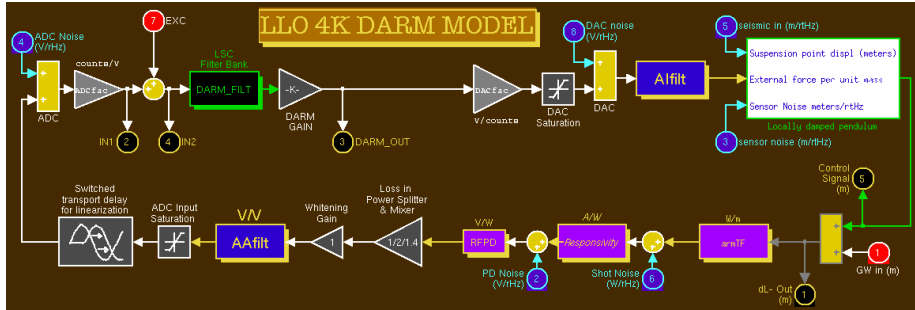


Figure 6: Control System Model created by Rana Adhikari. [6]

However, even with this stable system, any input into the inverted sensing function will exponentially blow up to infinity. This is due to the time delay within the sensing function. When inverted, the delay becomes a time advance, which is unphysical. The time advance creates poles with positive real parts.

Positive real poles are a problem because of the following equation:

$$y(t) = \sum_{i=1}^n C_i e^{p_i t} \quad (10)$$

where  $p_i$  is a pole in the Laplace  $s$ -plane. From this equation we see that the imaginary part of the pole determines the frequency of a response, and the real part determines the exponential growth. If the real part of a pole is positive, then the time response  $y(t)$  will blow up exponentially. This is what happened with our Simulink model.

To stop the exponential growth of the system, I simply removed the poles with positive real parts. This means my new inverse sensing function is now only an approximation. Figure 7 and 8 show the comparison between the calculated and physical models. For both, we have good agreement up until 1 kHz, where the downturn from the extra poles added at 8 kHz begin to take effect.

After these alterations to the inverse sensing function, we were finally able to reconstruct our input gravitational wave strain using Adhikari's model. [6] Figure 9 shows the comparison between the calculated and physical model's reconstruction at different frequencies. We wanted unity reconstruction, but found a gain in response surrounding 200 Hz and the dropoff due to the additional poles beginning at 1 kHz.

Potential solutions to these inconsistencies include adding in the poles at higher frequency and not removing the time advance poles. If we upsample the model prior to adding in the stability poles, we can add them at any frequency we want, as long as it is below the sampling frequency. If we add them at 16 kHz rather than 8 kHz, this could reduce the effect on the frequency response within the LIGO range.

For the unphysical time advance, rather than removing those poles and significantly altering our model, we might simply add in a delay that compensates

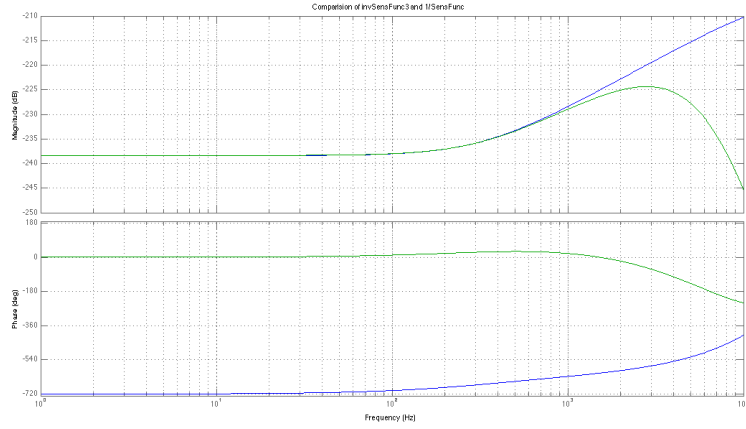


Figure 7: Inverse Sensing Function Calculated (Blue) and Physical (Green)

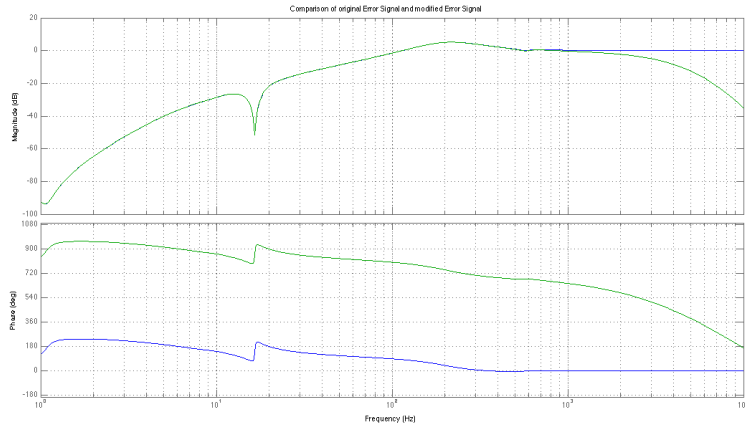


Figure 8: Inverse Sensing Function plus Error Signal Calculated (Blue) and Physical (Green)

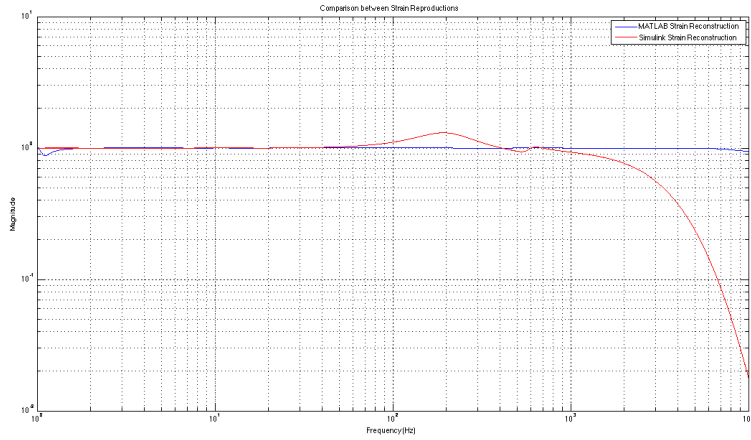


Figure 9: Calculated Strain Reconstruction (Blue) and Physical Strain Reconstruction (Red)

for the advance. This delay would make the positive real poles disappear in a way we can track and compensate for later in the frequency response.

### 3 Future Objectives

Instead of performing “downstream” calibrations, we hope to implement the calibration system within the digital control system, and thereby track the time changes of the component response functions more effectively. The calibration system will be built as a component of the control system at the Caltech 40m interferometer. To calibrate the detectors, calibration lines are injected into the system at known frequencies. The calibration lines’ response to the control loop are tracked, giving an idea of how noise and GW strain respond to the control loop in real time. Using this new method of calibration, we aim to accurately track the real-time changes in the detector response function, thus generating a faster, more reliable way of calculating gravitational wave strain.

The next step is to implement the calibration system to the Caltech 40m interferometer control system for testing. We will use the RCG (Real-time Code Generator) to take Simulink and MATLAB code and make C code from it. The ultimate goal is to implement the calibrator at the sites at Hanford and Livingston, tracking the parameters of the interferometers in real time.

### References

- [1] LIGO Scientific Collaboration (Abadie, J. et al.) Nucl.Instrum.Meth. A624 (2010) 223-240 arXiv:1007.3973 [gr-qc]

- [2] Siemens, X., et al., 2004. Making  $h(t)$  for LIGO. *Class. Quantum Grav.* 21 (S1723)
- [3] Abbott, B. P., et al., 2009. LIGO: The Laser Interferometer Gravitational-Wave Observatory. *Rep. Prog. Phys.* 72 (076901).
- [4] J. Kissel. *Calibrating and Improving the Sensitivity of the LIGO Detectors*. PhD thesis, Louisiana State University, 2010.
- [5] R. Adhikari. *Sensitivity and Noise Analysis of 4 km Laser Interferometric Gravitational Wave Antennae*. PhD thesis, Massachusetts Institute of Technology, 2004.
- [6] R. Adhikari. *LLO 4K DARM Model*. Simulink/MATLAB Model, California Institute of Technology, 2013.